



AIAA 99-0867

**Modeling the Effects of Weak
Ionization on Supersonic Flow and
Shock Waves**

Jonathan Poggie

US Air Force Research Laboratory

Wright-Patterson AFB, OH 45433-7913

**37th AIAA Aerospace Sciences
Meeting and Exhibit
January 11-14, 1999/Reno, NV**

Modeling the Effects of Weak Ionization on Supersonic Flow and Shock Waves

Jonathan Poggie*

US Air Force Research Laboratory
Wright-Patterson AFB, OH 45433-7913

Preliminary results are presented on the use of electromagnetic energy addition for hypersonic flow control. Several well-known analytical solutions of the equations of gasdynamics and magnetogasdynamics were used to study (separately) the relative importance of exothermic reactions, axial temperature variation, and an imposed magnetic field in the glow discharge tube experiments of Ganguly *et al.*¹ Of the three effects addressed, thermal nonuniformity appears to have the most influence on the experimental results. A detonation model can probably be ruled out for two reasons. First, insufficient energy is available from electron-ion recombination reactions to drive the detonation. Second, the detonation model predicts an increase in shock density ratio with increasing heat release, in contrast to the apparent drop seen in the experiments. In a similar manner, an ideal magnetohydrodynamic shock model can probably be ruled out for lack of adequate electrical conductivity and of a sufficiently strong imposed magnetic field. This conclusion does not, however, exclude other electromagnetic phenomena, and the issue of the apparent shock splitting has not been addressed here. A combination of careful temperature measurements and numerical simulations is required to determine whether thermal effects or physics inherent to the plasma are dominant in these experiments. It is evident, however, that all three of the mechanisms examined show promise for use in hypersonic flow control.

Nomenclature

Roman Symbols

A, B, C	coefficients of quadratic equation
a	sound speed
B	magnetic field strength
C_p	constant pressure specific heat
C_v	constant volume specific heat
h	enthalpy
H	nondimensional heat release parameter
I	current
J^\pm	Riemann invariants ($u \pm 2a/(\gamma - 1)$)
L	width of detonation wave system
M	Mach number
p	pressure
q	heat release parameter
Q	magnetic pressure parameter
r	radial distance
R	ideal gas constant (= 208.13 m ² /s ² /K for argon)
t	time
s	entropy
T	temperature
u	velocity
v	specific volume
W	shock or detonation speed
x	position

Greek Symbols

γ	adiabatic exponent (= 1.67 for argon)
μ_0	permeability of free space ($4\pi \times 10^{-7}$ N/A ²)
ρ	density
σ	electrical conductivity

Subscripts

d	detonation
f	formation
I	incident wave
R	reflected wave
T	transmitted wave

Introduction

EXTENSIVE experimental research has examined the effects of introducing weak, nonequilibrium ionization (fractional ionizations on the order of 10^{-8} to 10^{-6}) upstream of a shock. The speed, strength, and structure of the shock may be affected. In particular, reductions in heat transfer and drag have been claimed, based on the results of tests on wind tunnel models. (For recent, detailed bibliographies, see, for example, the conference proceedings of the Weakly Ionized Gas Workshops,^{2,3} the dissertation of Hilbun,⁴ and the paper by Adamovich *et al.*⁵) These experimental results have revived interest in using electromagnetic effects to control the flow over hypersonic

*Research Aerospace Engineer, Air Vehicles Directorate, AFRL/VAAC, 2645 Fifth Street, Suite 7. Member AIAA.

This paper is a work of the U.S. Government and is not subject to copyright protection in the United States.

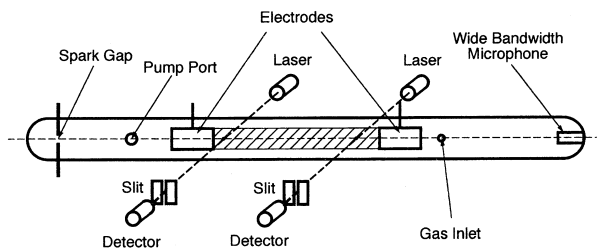


Fig. 1 Schematic diagram of experiments in glow discharge tube. From Ganguly *et al.*¹

air vehicles, where conventional means of control have a substantial penalty in increased heat transfer and vehicle weight.⁶

There is, however, continuing controversy over the causes and interpretation of the phenomena observed in the experiments.²⁻⁵ Researchers have variously attributed the changes in flow structure to a plasma-induced change in sound speed,⁷ streamer structures in microwave discharges,⁸ exothermic recombination reactions in the shock,⁹⁻¹¹ and temperature variation upstream of the shock.¹² Adamovich *et al.*⁵ have addressed the issue of the apparent shock splitting seen in the experiments, and have studied the conditions required for a steady-state, two-shock system to exist.

The present paper represents part of an ongoing study of the use of electromagnetic energy addition as a means for controlling the flow over a hypersonic vehicle. Preliminary work has addressed the implications of various mechanisms proposed to explain the experimental results. A wide variety of experiments in plasma aerodynamics have been reported, but here we will focus on a case first investigated by Klimov *et al.*,¹³ in which a shock was generated with an electrical discharge and propagated down a tube through an ionized region.

Ganguly *et al.*¹ recently carried out a set of well-documented experiments on this problem. A schematic diagram of the experimental apparatus is shown in Fig. 1. The tests were carried out in a 50 mm diameter Pyrex tube, which was roughly 1 m long and filled with argon gas. The pressure was fixed at about 4 kPa (30 torr) using a regulated purge flow. According to Hilbun,⁴ the mean velocity in the tube was on the order of 1 m/s. A shock was generated at the spark gap (left side of diagram, 272 mm from the start of the glow discharge) with an energy release of about 100 J. Downstream of the spark gap, a pair of 30 mm diameter cylindrical electrodes, separated by 300 mm, were used to generate a longitudinal plasma, with the cathode on the left in the diagram. The discharge was operated at constant current in the range 0 mA to 140 mA using a 10 kV, 300 mA direct current power supply.

The arrival of the shock pulse was recorded using a laser deflection technique at two stations located 302 mm and 422 mm from the spark gap in the pos-

itive column of the glow discharge. The lasers, slits, and photodetectors are shown schematically in Fig. 1. As the laser beam passes through the experimental apparatus, it is deflected by changes in index of refraction brought about by density variations. The slits in front of the photodetectors cut out a portion of the deflected beam so that the amount of light reaching the photodetectors is a function of the beam deflection. Thus, the signal recorded by the photodetectors corresponds to the derivative of density along the direction normal to the slits (i.e., along the tube), averaged over the optical path.

This averaging in the transverse direction has led to a controversy about whether to accept the apparent shock splitting observed by Ganguly *et al.* at face value⁵ or to attribute it to an averaging of a nonuniform flow by the optical diagnostic technique.⁴ For the present work, it will be assumed that only one shock is present in the pulse. The validity of this assumption will be examined by comparison of the calculations with the experimental data.

Calculated velocities will be compared to the average shock pulse velocity derived from measurements at two photodetector stations. It should be noted that the velocity of the shock pulse in the experiments is not expected to be constant over the relatively large distance between the detectors. Indeed, the pulse generated by a spark typically slows down as it expands and distributes its energy over a larger volume. The average velocity should, however, be suitable for comparison with the order of magnitude calculations described below.

An arrival time at each of the two photodetector stations was determined from the first rise above the ambient signal discernible by eye in the time-series plots in Ganguly *et al.*¹ The average velocity of the shock pulse between the two stations was determined by dividing the distance between stations (120 mm) by the difference in arrival time. The results are shown in Fig. 2 as a function of discharge current. The average velocity is seen to rise from an initial value of about 470 m/s with no current flowing to about 640 m/s at $I = 140$ mA.

An increase in shock velocity with increased current is expected because of the increase in the neutral gas temperature from Joule heating in the region between the two electrodes. An assessment of the non-thermal effects present in the experiments depends on how accurately the temperature field in the experiment is known. Unfortunately, temperature measurements are not available for the glow discharge experiments, so a temperature calculation is necessary to quantitatively compare shock speed computations to the experiments.

To this end, Hilbun⁴ carried out a steady-state, axisymmetric heat conduction computation with a Joule heating source term. He solved a nonlinear ordinary

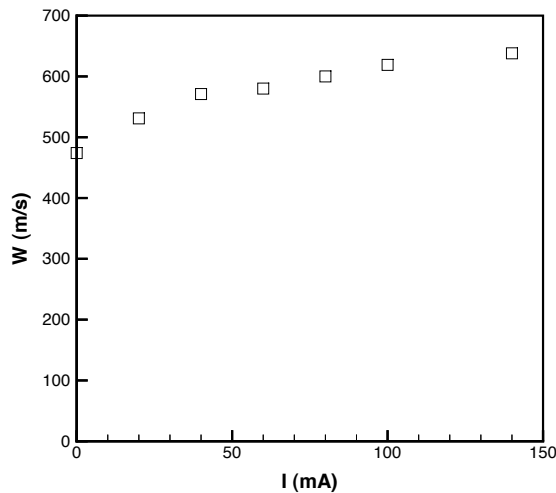


Fig. 2 Average shock pulse velocity derived from laser deflection measurements in the glow discharge tube. Derived from the data of Ganguly *et al.*¹

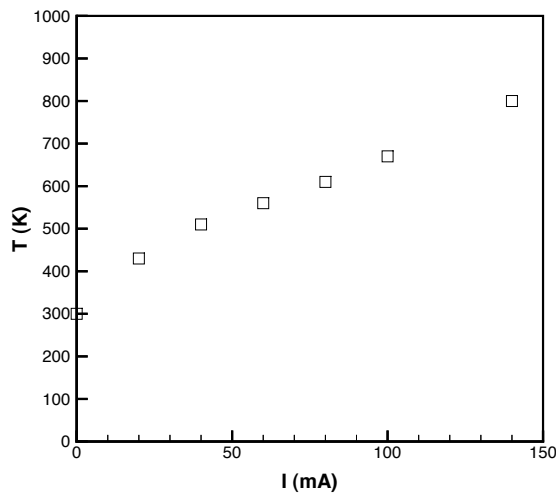


Fig. 3 Calculated temperature, averaged across the tube cross-section, for the glow discharge experiments. Data from Hilbun.⁴

differential equation using a fourth order Runge-Kutta shooting method to obtain the radial temperature profile in the region of the glow discharge and the corresponding average across the cross-section. Although this model neglects, among other things, convection and radiation, it had to be used in the calculations for lack of direct measurements.

The computed temperature, averaged across the cross-section of the tube, is shown as a function of discharge current in Fig. 3. The mean temperature increases from an assumed room temperature of 300 K with current off to nearly 800 K at the maximum current of 140 mA.

The following sections will examine the relative im-

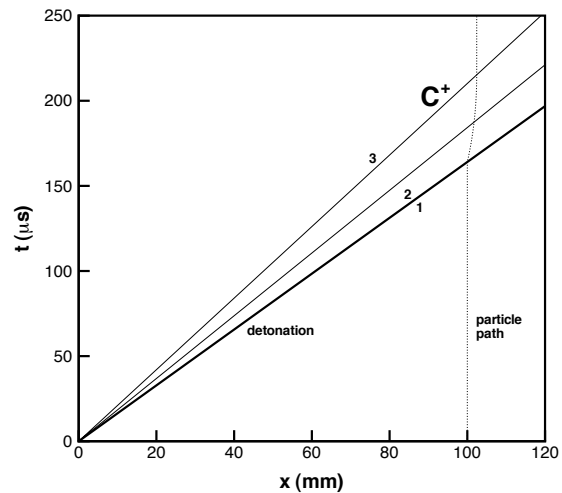


Fig. 4 Detonation/expansion system on a space-time diagram. Origin represents point where incident shock ignites detonation. Conditions: argon with $T_1 = 600$ K and $q = 20$ kJ/kg.

portance in the glow discharge experiments of exothermic reactions, axial temperature variation, and an imposed magnetic field. For each of these mechanisms, an analytical model will be used to make an order of magnitude estimate of the conditions that would be required for that mechanism (acting alone) to explain the experimental observations. This work is intended to provide a theoretical context for discussion of the relative importance of these three effects, and to identify a path for more detailed numerical simulations.

Exothermic Reactions

One proposed explanation for the effects observed in the plasma aerodynamics experiments is heat release through exothermic reactions as the gas relaxes from a nonequilibrium state.^{9-11, 13, 14} The basic idea is that increased species concentration downstream of the shock causes recombination reaction rates to be greatly increased, driving the state closer to equilibrium and releasing chemical energy. In order for this explanation to be plausible, sufficient energy must be stored in the excited gas and adequate time must be available to release it. In the present section, these questions will be addressed for the glow discharge tube experiment by using a one-dimensional analytical model to make order of magnitude estimates of the required energy and time.

Here it will be assumed that the problem of the shock propagating in a glow discharge is analogous to a shock-ignited detonation:¹⁵ the spark generates a shock pulse that enters the ionized region, ignites an exothermic reaction, and develops into a detonation moving at constant velocity W trailed by an unsteady expansion wave. The detailed solution to this problem was apparently first considered by Taylor.¹⁶ It is es-

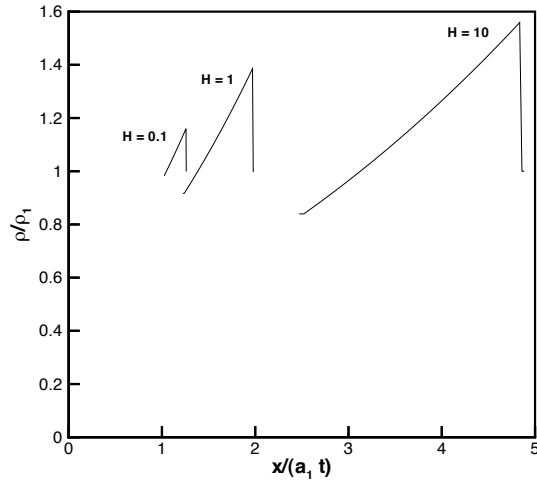


Fig. 5 Density profiles through a detonation/expansion wave system traveling in argon.

essentially a standard centered expansion fan with one uniform region replaced by the detonation wave.

Following Taylor, we solve the one-dimensional Euler equations for homentropic flow using the method of characteristics (see Thompson¹⁷). The form assumed for the detonation/expansion system is shown on the space-time diagram of Fig. 4. The origin corresponds to the point of ignition of the detonation. The detonation wave is indicated by a heavy line in the diagram with slope $1/W$. It compresses the initially undisturbed gas from State 1, where the velocity u is zero, to State 2, which is the beginning of the expansion. For a steady detonation, the first characteristic of the expansion wave (State 2) is required to move at the detonation velocity: $u_2 + a_2 = W$. The resulting flow then expands continuously down to State 3, where the velocity must return to zero to match the boundary condition at the closed end of the tube. The expansion is a simple region,¹⁷ so that the J^+ characteristics appear in the figure as straight lines from the origin with constant slope $1/(u + a)$.

Using the fact that the J^- characteristics have the same value everywhere ($J^- = u - 2a/(\gamma - 1) = \text{const}$), and using the conditions downstream of the detonation (State 2) as a reference, we solve for the sound speed as a function of position and time:

$$\frac{a}{a_2} = 1 + \frac{\gamma - 1}{\gamma + 1} \left(\frac{x}{a_2 t} - \frac{W}{a_2} \right) \quad (1)$$

The pressure and density ratios can be found from the assumption of isentropic flow: $p/p_2 = (a/a_2)^{2\gamma/(\gamma-1)}$ and $\rho/\rho_2 = (a/a_2)^{2/(\gamma-1)}$. The velocity is given by:

$$\frac{u}{a_2} = -1 + \frac{\gamma - 1}{\gamma + 1} \frac{W}{a_2} + \frac{2}{\gamma + 1} \frac{x}{a_2 t} \quad (2)$$

The jump conditions across the detonation are now needed to complete the solution.

As a simple model for the detonation, we will use the well-known approximation of an ideal gas normal shock in which the difference in zero-point enthalpy $q = h_{f1} - h_{f2}$ is taken to be a known constant.¹⁷⁻¹⁹ The adiabatic exponent γ is assumed to be remain constant across the shock. With the absolute enthalpy as $h = C_p T + h_f$, the difference in enthalpy between the upstream and downstream states becomes:

$$h_2 - h_1 = -q + C_p(T_2 - T_1) \quad (3)$$

The introduction of these assumptions and the ideal gas equation of state into the usual normal shock jump conditions for mass, momentum, and energy conservation (see Thompson¹⁷) leads to a Hugoniot equation of the form:

$$\frac{p_2}{p_1} = \left[2H + \frac{\gamma + 1}{\gamma - 1} - \frac{v_2}{v_1} \right] / \left[\frac{\gamma + 1}{\gamma - 1} \frac{v_2}{v_1} - 1 \right] \quad (4)$$

where $H = q\rho_1/p_1$ is a nondimensional heat release parameter. The corresponding Rayleigh line has the form:

$$\frac{p_2}{p_1} = 1 - \gamma M_d^2 \left(\frac{v_2}{v_1} - 1 \right) \quad (5)$$

where $M_d = W/a_1$ is the detonation Mach number. For the present problem of a wave system propagating in a tube of reactive material, we take the the upstream thermodynamic state as specified and calculate the detonation Mach number. Assuming a Chapman-Jouget detonation, where the Rayleigh line is tangent to the Hugoniot curve, there is a unique solution to this problem. By equating the derivatives of Eq. (4) and Eq. (5), and manipulating the results, we can find the specific volume ratio for the Chapman-Jouget detonation that occurs for a given level of heat release:

$$\frac{v_2}{v_1} = 1 + \frac{\gamma - 1}{\gamma} H - \frac{1}{\gamma} \sqrt{2\gamma \frac{\gamma - 1}{\gamma + 1} H + (\gamma - 1)^2 H^2} \quad (6)$$

This specific volume ratio can be substituted back into the Hugoniot equation (4) to obtain the corresponding pressure ratio. The detonation Mach number is:

$$M_d^2 = 1 + \frac{\gamma^2 - 1}{\gamma} H + \frac{\gamma + 1}{\gamma} \sqrt{2\gamma \frac{\gamma - 1}{\gamma + 1} H + (\gamma - 1)^2 H^2} \quad (7)$$

Figure 5 shows the density profile through the detonation and expansion wave system for three values of the nondimensional heat release parameter. The density profile can be interpreted as a ‘snapshot’ of a sawtooth waveform traveling from left to right. As the wave system overtakes the undisturbed gas, a particle of fluid first encounters the jump in density at the detonation front (right side of each waveform). From there the fluid is carried to the right until the flow expands down to zero velocity at the end of the expansion (left

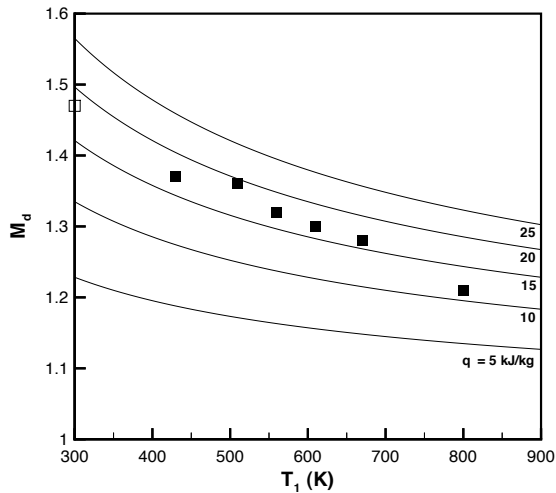


Fig. 6 Detonation Mach number as a function of upstream temperature and heat release. Symbols: average Mach number derived from the data of Ganguly *et al.*¹ using the temperature calculations of Hilbun.⁴

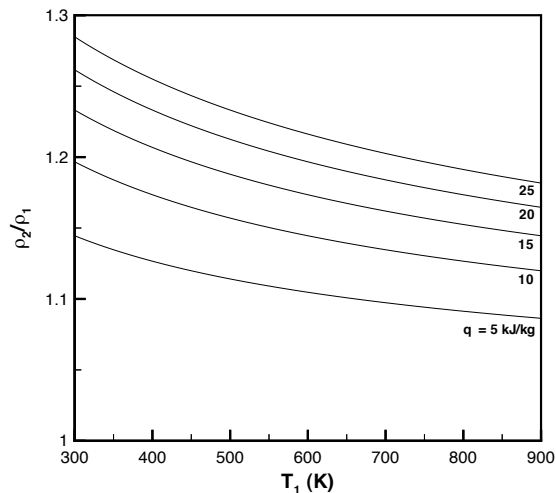


Fig. 7 Detonation density ratio as a function of temperature and heat release.

side of each waveform). The wave system leaves behind a region of still gas with higher pressure and lower density than the ambient conditions upstream.

With the upstream conditions held constant, the Mach number, pressure ratio, and density ratio of the detonation increase with increasing dimensional chemical energy release (Eqs. (6) and (7)). These changes lead to the increases in the speed, width, and amplitude of the density waveform visible in the figure.

The predicted detonation Mach number from Eq. (7) is shown in Fig. 6 as function of upstream temperature for different levels of the dimensional heat release parameter. As noted above, the detonation Mach

number increases with heat release if the upstream temperature is held fixed. For a constant value of the dimensional heat release, however, the nondimensional heat release parameter decreases with increasing temperature. Thus the detonation Mach number decreases with increasing temperature for a given level of heat release, although the dimensional velocity does increase.

The average velocities between the two photodetector stations, converted to Mach numbers according to Hilbun's predictions of the temperature averaged over the cross-section, are shown as square symbols in the figure. Increasing temperature corresponds to increasing current in the experiment (see Fig. 3).

The experimental data appear to be consistent with a detonation sustained by a heat release of 15–20 kJ/kg, independent of the current. If the detonation were sustained by the energy stored in the nonequilibrium plasma, one would expect increased heat release with increased current in the glow discharge.

Note also the case with no plasma, indicated by a hollow symbol in the figure. No detonation will exist for this case; it represents the incident, spark-driven shock. The only requirement for this case in the present model is that the dimensional velocity of the detonation be higher than that of the incident shock so that the detonation pulse can develop. This is satisfied for the present data, but it is interesting that the zero-current case appears to lie on the same curve as the other data. The trend looks thermal.

A decrease in the amplitude of the laser deflection signal with increased discharge current was observed in the experiments. This decrease in amplitude could be caused by both a decrease in the derivative of the density along the axial direction and by the averaging of a nonuniform density field across the transverse direction.⁴ If the former effect is the most significant, it indicates a decrease in shock strength with increased discharge current. The model predicts a decrease in detonation density ratio with increased temperature at fixed heat release (Fig. 7), but an *increase* in density ratio with increased heat release at fixed upstream temperature. As mentioned above, one would expect in the context of the detonation model that more energy would be available to drive the detonation as the discharge current was increased.

The exothermic reactions must complete rapidly for a steady detonation wave system to exist. An upper bound on the required time is the residence time of a particle in the wave system.

At a given instant in time, the wave system has a distinct width L , the distance from the detonation to the trailing edge of the expansion. The detonation travels with speed W , while the trailing edge travels with the local sound speed a_3 . Using $u_2 = W - a_2$ and Eq. (1), it can be shown that $L = (\gamma + 1)/2 u_2 t$.

The path of a particle starting at a position x_0 can be found by solving the equation $dx/dt = u(x, t)$, using the velocity giving by Eq. (2). The solution $x(x_0, t)$ can be used to determine the time interval between when the detonation initially crosses a given fluid particle and when the particle exits the wave system. The time interval Δt is:

$$\Delta t = \frac{x_0}{W} \left\{ \left[\frac{\gamma + 1}{2} - \frac{\gamma - 1}{2} \frac{W}{a_2} \right]^{-\frac{\gamma+1}{\gamma-1}} - 1 \right\} \quad (8)$$

As an example, consider an initial particle position of $x_0 = 100$ mm, an upstream temperature of $T_1 = 600$ K, and a heat release of $q = 20$ kJ/kg (see Fig. 4). In this case, the detonation reaches the particle at about $160 \mu\text{s}$, where the width of the ‘sawtooth’ is about 20 mm, and the residence time is about $50 \mu\text{s}$. The reaction must take place within the detonation in a fraction of this time, say on the order of $10 \mu\text{s}$ or less. Otherwise, the reaction zone will be so thick that interaction with the wall boundary layer will quench the detonation.¹⁸

Thermal Effects

This section will address the issue of thermal nonuniformity along the axial direction in the glow discharge tube experiments. The electric current flowing between the two electrodes in the experiments generates heat (Joule heating) that is carried away by conduction and convection due to the slow purge of the working fluid. These processes should produce a roughly axisymmetric temperature distribution $T(x, r)$ in the tube.

With detailed measurements of the temperature field, it should be possible to do a fairly accurate numerical simulation of the baseline thermal effects, as Hilbun⁴ did with a calculated temperature distribution. Here we will not attempt to replicate Hilbun’s computation, but rather to understand the phenomena associated with thermal inhomogeneity. For simplicity, the thermal variations will be modeled as a contact surface located at the right of the first electrode (lumping all the x -dependence at the contact surface, and averaging out the r -dependence). The trailing expansion system of the spark-driven shock will be neglected. Some of the realism of the model is lost with these assumptions, but they make it possible to utilize analytical solutions.

As a first model, we will assume that the only thermal nonuniformity is in the axial direction, and consider the case of a plane shock impinging at normal incidence on a plane contact surface. Early theoretical treatments of this problem were carried out by Paterson²⁰ and by Courant and Friedrichs.²¹ A detailed experimental and theoretical study was done by Ford and Glass.^{22, 23}

The problem is illustrated in the space-time diagram of Fig. 8. The numbers designate regions of uniform

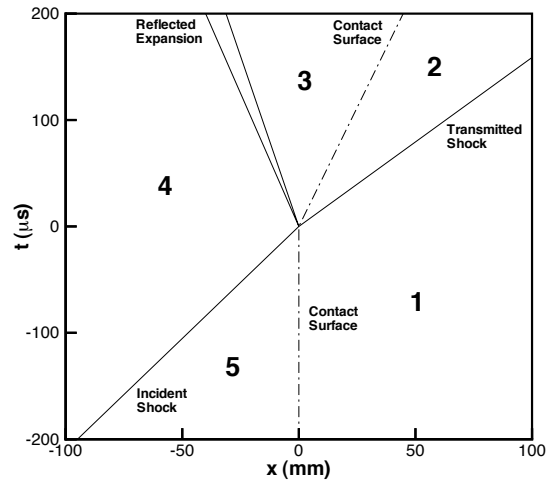


Fig. 8 Space-time diagram for normal reflection of a shock at a contact surface in argon ($M_I = 1.47$, $T_5 = 300$ K, $T_1 = 600$ K).

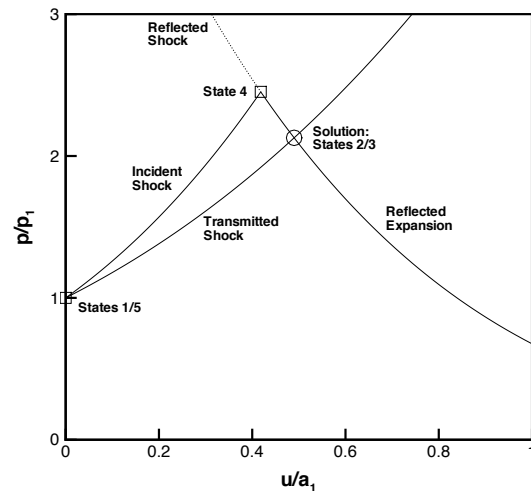


Fig. 9 Pressure-velocity diagram for normal reflection of a shock at a contact surface in argon ($M_I = 1.47$, $T_1/T_5 = 2$).

flow. For $t < 0$, the incident shock propagates to the right in the diagram toward a stationary contact surface which separates two still fluids at a given pressure (regions 1 and 5). Behind the shock lies a region (4) of uniform rightward flow at higher pressure. At $t = 0$, the shock hits the contact surface, generating transmitted and reflected waves. The transmitted wave is always a shock, but the reflected wave can be either a shock or a centered expansion fan, depending on the generalized acoustic impedance ratio of the contact surface. For the case under consideration here, where the gas on both sides of the contact surface is the same and the temperature is higher on the right, the reflected wave is an expansion. The initial and final

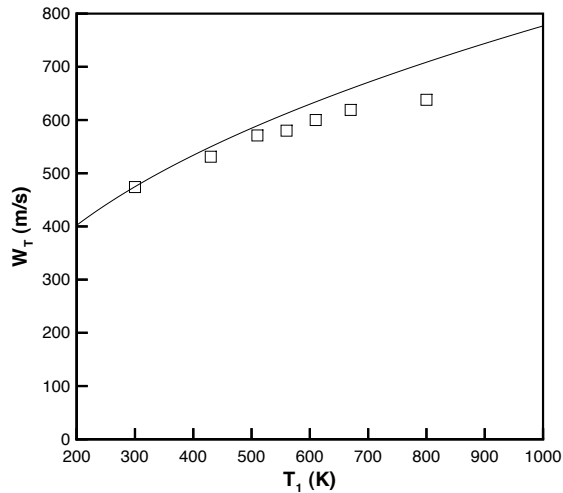


Fig. 10 Contact surface model of glow discharge experiment. Solid line: transmitted wave speed for $M_I = 1.47$ and $T_5 = 300$ K in argon. Symbols: Data of Ganguly *et al.*¹ reduced according to the calculations of Hilbun.⁴

characteristics of the expansion fan are shown in the figure, bounding a nonuniform region that separates regions 3 and 4.

Two new regions (2 and 3) appear between the reflected and transmitted waves. Again, the pressure and velocity both match across the contact surface. The flow in these regions carries the contact surface to the right.

The problem was solved by applying the secant method to finding the roots of the implicit equations of Ford and Glass.²³ A sample result is indicated by a circle in Fig. 9, along with a graphical solution. State 1, state 5, and the strength of the incident shock are taken as given. The problem is solved by choosing a reflected expansion and a transmitted shock such that the pressure and velocity match on both sides of the contact surface.

The incident shock connects state 5 to state 4. These states are shown in the diagram as square symbols connected by a curve representing all the possible downstream states of right-running shocks with upstream state 5. In a similar fashion, all the possible transmitted shocks are shown originating at state 1 (coincident with state 5 on the diagram). From state 4 are shown all the possible reflected expansions and reflected shocks. The solution, representing states 2 and 3, is found at the intersection of the curves for the transmitted shock and reflected expansion. The computed solution, marked by a circle, lies at that point. The transmitted shock has a higher velocity (Fig. 8) and a lower strength (Fig. 9) than the incident shock, consistent with the observations in the glow discharge experiments.

Fig. 10 shows the application of the model to the

experiment of Ganguly *et al.*,¹ again using average velocities and the calculated temperature profile, averaged over the tube cross-section.⁴ The point corresponding to a temperature of 300 K represents the case with zero current in the experiment. Here there is no contact surface because there is no axial temperature variation, so this point was used to determine the strength of the incident shock. For completeness, temperatures both lower (reflected shock) and higher (reflected expansion) are shown. Despite the simplifying assumptions made in the present analysis, the contact surface model seems to be a fair estimate of the trends seen in the experimental data.

Applied Magnetic Field

Purely electromagnetic effects are another possible mechanism for the results observed in the glow discharge tube experiments. Both Hilbun⁴ and Adamovich *et al.*⁵ have examined the issue of charge separation in the shock, and have concluded that this mechanism has little effect on the flow for the weak ionization present in the experiments. Here we address another possibility: the effect of an imposed magnetic field, such as that generated by the current flowing in the glow discharge.

The issue of an imposed magnetic field has been examined experimentally. Gorshkov *et al.*²⁴ extended the work of Klimov *et al.*¹³ to include an applied magnetic field. They observed a reduction in shock wave velocity with increased strength of a transverse magnetic field. A longitudinal field had almost no effect on the shock.

The additional complexity introduced by the magnetic body force makes it difficult to carry out an analysis similar to those described above for exothermic reactions and axial temperature variation. Here we will simply use the shock Mach number based on the average velocity in the experiments of Ganguly *et al.* and determine whether a plausible value for the imposed magnetic field can cause a significant reduction in the density ratio across the shock.

We will take as a model problem a plane magnetohydrodynamic shock wave in which the magnetic field is oriented perpendicular to the flow direction. (These assumptions restrict the possible solutions to the ‘fast’ shock, excluding the ‘slow’ shock and the Alfvén shock.) The electrical conductivity will be taken to be infinite (ideal magnetohydrodynamics). The jump conditions for ideal magnetohydrodynamic shocks were first derived by de Hoffmann and Teller,²⁵ and are treated in detail in standard references on magnetohydrodynamics.^{26–28}

The equation of mass conservation remains the same as for an ordinary gasdynamic shock:

$$\rho_2(W - u_2) = \rho_1 W \quad (9)$$

where state 1 represents the undisturbed fluid, state 2

lies behind the shock, W is the shock speed, and u_2 is the particle speed behind the shock. The magnetic body force adds a term to the momentum equation that is equivalent to an additional effective pressure $B^2/(2\mu_0)$:

$$\frac{p_2 + \rho_2(W - u_2)^2 + B_2^2/(2\mu_0)}{p_1 + \rho_1 W^2 + B_1^2/(2\mu_0)} = \quad (10)$$

Similarly, a new term $B^2/(\rho\mu_0)$ appears in the energy jump relation:

$$\frac{h_2 + (W - u_2)^2/2 + B_2^2/(\rho_2\mu_0)}{h_1 + W^2/2 + B_1^2/(\rho_1\mu_0)} = \quad (11)$$

An entirely new jump condition is derived from the magnetic induction equation:

$$(W - u_2)B_2 = WB_1 \quad (12)$$

As for an ordinary gasdynamic shock, the velocity in the shock reference frame decreases across a magnetohydrodynamic shock, so Eq. (12) requires that the magnetic field increase. A corresponding current sheet must exist coincident with the shock in order to satisfy Ampère's law. The jump conditions are supplemented by the second law restriction that the entropy cannot decrease across the shock: $s_2 \geq s_1$.

Assuming an ideal ($p = \rho RT$), thermally perfect ($h = C_p T$) gas, and manipulating Eq. (9) through Eq. (12), we find a quadratic equation for the density ratio across the shock:

$$A \left(\frac{\rho_2}{\rho_1} \right)^2 + B \left(\frac{\rho_2}{\rho_1} \right) + C = 0 \quad (13)$$

where

$$A = Q(2 - \gamma) \quad (14)$$

$$B = \gamma(Q + 1) + \gamma M_1^2(\gamma - 1)/2 \quad (15)$$

$$C = -\gamma M_1^2(\gamma + 1)/2 \quad (16)$$

and $Q = B_1^2/(2\mu_0 p_1)$ is the ratio of the effective magnetic pressure to the gas pressure on the upstream side of the shock. The shock density ratio is seen to be a function of the Mach number M_1 and the nondimensional magnetic field strength Q .

For $\gamma < 2$, which is satisfied for ideal gases, there is one positive and one negative root of Eq. (13). Only the positive root is physically relevant.²⁶

To make at least a qualitative comparison with the glow discharge tube experiments, we take argon at $p_1 = 4$ kPa, and consider Mach numbers in the range observed in the experiments: $1.2 \leq M_1 \leq 1.5$. Figure 11 shows the effect of varying the upstream magnetic field strength. A significant decrease in the shock density ratio is obtained for an imposed magnetic field strength on the order of 10^{-2} T.

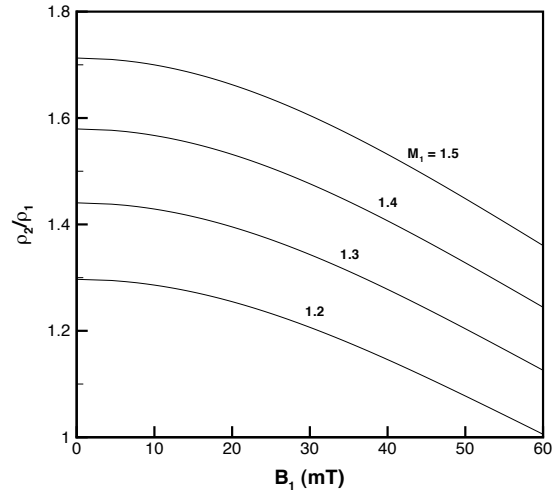


Fig. 11 Density ratio across a magnetohydrodynamic shock as a function of magnetic field strength for several different Mach numbers ($p_1 = 4$ kPa).

One possible objection to the magnetohydrodynamic shock model is that, for relatively low values of the electrical conductivity, the magnetic Reynolds number of the flow will be low, and the problem will more closely resemble a gasdynamic shock embedded in a magnetohydrodynamic channel flow. The basic parameter in question is the thickness of the magnetohydrodynamic shock relative to the dimensions of the experiment.

The problem of magnetohydrodynamic shock for a transverse magnetic field was solved by Marshall,²⁹ but an order of magnitude estimate of the thickness of the transition layer for the magnetic field is simply $1/(\mu_0 \sigma W)$.²⁶ The conductivity required to obtain a thickness on the order of 10 mm with $W = 600$ m/s is on the order of $\sigma = 10^5/(\Omega \cdot \text{m})$, a rather large value. This issue merits detailed study with finite-conductivity numerical calculations.

Summary and Concluding Remarks

Several well-known analytical solutions of the equations of gasdynamics and magnetogasdynamics were used to study the effects of exothermic reactions, axial temperature variation, and an imposed magnetic field in the glow discharge tube experiments of Ganguly *et al.*¹ The work addressed some of the same issues as some other recent studies,^{4,5} but from a different perspective.

Two somewhat questionable methods of reducing the experimental data had to be used so that they could be compared to the present calculations. First, the mean temperatures computed by Hilbun⁴ were used for lack of detailed temperature measurements. Second, an average velocity was constructed using data from two widely-separated (120 mm apart) stations. These assumptions are believed to introduce

error comparable to that inherent in applying the idealized analytical models used in the calculations. The results presented here should therefore be viewed as order of magnitude estimates. More detailed experiments are currently underway, so these issues can be addressed in future work.

The first issue examined was the effect of the exothermic reactions that occur as the nonequilibrium, ionized gas relaxes downstream of the shock. The experimental data appear to be consistent with a steady-state detonation sustained by a heat release on the order of 10 kJ/kg in less than 10 μ s, independent of the current. If a detonation were driven by relaxation from a nonequilibrium state, the heat release would be expected to increase with increasing current in the glow discharge and the concomitant increase in the energy supplied to the nonequilibrium state. Further, an energy release on the order of 10 kJ/kg seems excessively large given the limited amount of energy that could be stored in the weakly ionized gas. With an ionization energy of 38 MJ/kg (15.8 eV/atom) and a fractional ionization of 10^{-6} , less than 40 J/kg would be available to drive the detonation. For the detonation model to apply, the required energy would have to be stored in some form other than the chemical energy of ionization.

A qualitative difference between the detonation model and the experimental results was also present. All other things being equal, increasing energy release increases the speed and strength of a detonation pulse in a shock tube. In contrast, increased speed but apparently decreased strength of a shock pulse were observed as the current, and presumably the energy available for release, were increased in the glow discharge experiments.

It should be noted that the one-dimensional model used here does not include the complex cellular structure and turbulence that are often present in detonations traveling in combustible materials. These phenomena are obviously beyond the scope of the models used in this paper, but they can be treated through numerical simulation.

The issue of thermal nonuniformity was addressed through a model in which the axial temperature variation was lumped as a contact surface at the start of the glow discharge. The contact surface model showed qualitative agreement with the observed reduction in shock strength and impressively good quantitative agreement with the reduced experimental data. The issue of thermal nonuniformity needs to be reviewed in more detail, however. The model assumed a flat shock incident on a flat contact surface. In the experiments, the spark-generated shock was almost certainly accompanied by a trailing expansion fan, and the temperature must have varied smoothly in the radial and axial directions. The results also depend on the mean temperature, which was calculated and

not measured.

In ongoing work, thermal variations are being explored more fully through numerical solutions of the two-dimensional Euler equations. Combined with careful temperature measurements in the glow discharge, this approach should be able to accurately treat the baseline thermal effects present in the experiments.

Finally, the issue of an imposed magnetic field was examined with a magnetohydrodynamic shock model. A magnetic field strength on the order of 10 mT (100 G) had significant effect on the shock density ratio. The required magnetic field is controlled primarily by the ambient pressure, which sets the magnitude of the nondimensional parameter Q . The current in the glow discharge should set up a region of approximately circumferential magnetic field lines, which are tangent to the shock as assumed in the model, but this field is probably not as strong as 10 mT. For comparison, a current of 100 mA through a straight wire induces a magnetic field of $B = \mu_0 I / (2\pi r) \approx 1 \mu\text{T}$ at $r = 30$ mm from the wire. Further, the electrical conductivity in the glow discharge is probably not high enough to support a magnetohydrodynamic shock. This issue needs to be reexamined with finite-conductivity numerical calculations.

Of the three effects addressed in this paper, thermal nonuniformity probably has the most influence on the experimental results. The detonation model can be ruled out unless there is both a source of energy other than electron-ion recombination to drive the detonation and the inference from the laser deflection signal of reduced shock density ratio is incorrect. In a similar manner, the magnetohydrodynamic shock model can be ruled out for lack of adequate electrical conductivity and of a sufficiently strong imposed magnetic field. This conclusion does not rule out other electromagnetic phenomena, however. The issue of the apparent shock splitting has not been addressed here. A combination of careful temperature measurements and numerical computations should be able to determine whether thermal effects are the whole story or physics inherent to the plasma are important.

All three physical mechanisms examined in this paper do show promise for use in hypersonic flow control. Considerably greater amounts of energy can be stored in nonequilibrium air than in the weak ionization present in the argon experiments. The laser spike concept, an example of straight heat addition, has already been demonstrated,^{30,31} as has a low magnetic Reynolds number magnetohydrodynamic flow control system.³² A clear path has been identified for future work, and electromagnetic energy addition shows great promise for controlling of hypersonic flow.

Acknowledgments

This project was sponsored by the Air Force Office of Scientific Research, and monitored by M. Jacobs and S. Walker. This work is being carried out in collaboration with D. Gaitonde, E. Josyula, J. Schmisser, and J. Shang. The author would like to acknowledge helpful discussions of the present work with W. Bailey, A. Creese, and R. Kimmel.

The L^AT_EX class file used to generate this paper was written by W. Kleb of NASA Langley Research Center, and is available from:

<http://abftp.larc.nasa.gov:8080/~kleb/aiaa/>

References

- ¹Ganguly, B. N., Bletzinger, P., and Garscadden, A., "Shock Wave Damping and Dispersion in Nonequilibrium Low Pressure Argon Plasmas," *Physics Letters A*, Vol. 230, 1997, pp. 218–222.
- ²Bain, W. L., editor, *Proceedings of the 1st Workshop on Weakly Ionized Gases*, 2 vols., Wright Laboratory Aero Propulsion and Power Directorate, Wright-Patterson AFB, OH, June 1997.
- ³Bain, W. L., editor, *Proceedings of the 2nd Workshop on Weakly Ionized Gases*, AIAA, Washington, DC, April 1998.
- ⁴Hilbun, W. M., *Shock Waves in Nonequilibrium Gases and Plasmas*, Ph.D. thesis, Air Force Institute of Technology, Wright-Patterson AFB, OH, October 1997.
- ⁵Adamovich, I. V., Subramaniam, V. V., Rich, J. W., and Macheret, S. O., "Phenomenological Analysis of Shock-Wave Propagation in Weakly Ionized Plasmas," *AIAA Journal*, Vol. 36, No. 5, 1998, pp. 816–822.
- ⁶Gurijanov, E. P. and Harsha, P. T., "AJAX: New Directions in Hypersonic Technology," AIAA Paper 96-4609, November 1996.
- ⁷Mishin, G. I., "Sound and Shock Waves in a Gas Discharge Plasma," *Proceedings of the 1st Workshop on Weakly Ionized Gases*, Vol. 1, Wright Laboratory Aero Propulsion and Power Directorate, Wright-Patterson AFB, OH, June 1997, pp. E-1 – E-12.
- ⁸Khodataev, K. V., "Physics of Under-Critical Microwave Discharge and Its Influence on Supersonic Aerodynamics and Shock Waves," *Proceedings of the 1st Workshop on Weakly Ionized Gases*, Vol. 1, Wright Laboratory Aero Propulsion and Power Directorate, Wright-Patterson AFB, OH, June 1997, pp. L-1 – L-12.
- ⁹Bychkov, V., "Theoretical Analysis of Plasma Aerodynamic Experiments," *Proceedings of the 1st Workshop on Weakly Ionized Gases*, Vol. 1, Wright Laboratory Aero Propulsion and Power Directorate, Wright-Patterson AFB, OH, June 1997, pp. I-1 – I-18.
- ¹⁰Kelley, J. D., "Studies of Flow Phenomena in Ionized Gases," *Proceedings of the 1st Workshop on Weakly Ionized Gases*, Vol. 1, Wright Laboratory Aero Propulsion and Power Directorate, Wright-Patterson AFB, OH, June 1997, pp. V-1 – V-18.
- ¹¹Zaslanko, I. S., "Non-Equilibrium Kinetic Effects in Shock Waves," *Proceedings of the 1st Workshop on Weakly Ionized Gases*, Vol. 1, Wright Laboratory Aero Propulsion and Power Directorate, Wright-Patterson AFB, OH, June 1997, pp. N-1 – N-52.
- ¹²Bailey, W. F. and Hilbun, W. M., "Baseline of Thermal Effects on Shock Propagation in Glow Discharges," *Proceedings of the 1st Workshop on Weakly Ionized Gases*, Vol. 2, Wright Laboratory Aero Propulsion and Power Directorate, Wright-Patterson AFB, OH, June 1997, pp. GG-1 – GG-18.
- ¹³Klimov, A. I., Koblov, A. N., Mishin, G. I., Serov, Y. L., and Yavor, I. P., "Shock Wave Propagation in a Glow Discharge," *Soviet Technical Physics Letters*, Vol. 8, No. 4, 1982, pp. 192–194.
- ¹⁴Vstovskii, G. V. and Kozlov, G. I., "Propagation of Weak Shock Waves in a Vibrationally Excited Gas," *Soviet Physics: Technical Physics*, Vol. 31, No. 8, 1986, pp. 911–914.
- ¹⁵Gaydon, A. G. and Hurle, I. R., *The Shock Tube in High-Temperature Chemical Physics*, Reinhold, New York, 1963.
- ¹⁶Taylor, G. I., "The Dynamics of the Combustion Products Behind Plane and Spherical Detonation Fronts in Explosives," *Proceedings of the Royal Society of London A*, Vol. 200, 1950, pp. 235–247.
- ¹⁷Thompson, P. A., *Compressible-Fluid Dynamics*, self-published, 1988, originally published by McGraw-Hill, 1972.
- ¹⁸Williams, F. A., *Combustion Theory: The Fundamental Theory of Chemically Reacting Flow Systems*, 2nd ed., Addison-Wesley, Redwood City, CA, 1985.
- ¹⁹Landau, L. D. and Lifshitz, E. M., *Fluid Mechanics*, 2nd ed., Pergamon Press, Oxford, 1987.
- ²⁰Paterson, S., "The Reflection of a Plane Shock Wave at a Gaseous Interface," *The Proceedings of the Physical Society*, Vol. 61, No. 2, 1948, pp. 119–121.
- ²¹Courant, R. and Friedrichs, K. O., *Supersonic Flow and Shock Waves*, Interscience, New York, 1948.
- ²²Glass, I. I. and Patterson, G. N., "A Theoretical and Experimental Study of Shock-Tube Flows," *Journal of the Aeronautical Sciences*, Vol. 22, No. 2, 1955, pp. 73–100.
- ²³Ford, C. A. and Glass, I. I., "An Experimental Study of One-Dimensional Shock-Wave Refraction," *Journal of the Aeronautical Sciences*, Vol. 23, No. 2, 1956, pp. 189–191.
- ²⁴Gorshkov, V. A., Klimov, A. I., Koblov, A. N., Mishin, G. I., Khodataev, K. V., and Yavor, I. P., "Propagation of Shock Waves in a Glow Discharge Plasma in the Presence of a Magnetic Field," *Soviet Physics: Technical Physics*, Vol. 29, No. 5, 1984, pp. 595–597.
- ²⁵de Hoffmann, F. and Teller, E., "Magneto-Hydrodynamic Shocks," *Physical Review*, Vol. 80, No. 4, 1950, pp. 692–703.
- ²⁶Ferraro, V. C. A. and Plumpton, C., *An Introduction to Magneto-Fluid Mechanics*, Oxford University Press, Oxford, 1961.
- ²⁷Sutton, G. W. and Sherman, A., *Engineering Magnetohydrodynamics*, McGraw-Hill, New York, 1965.
- ²⁸Jeffrey, A., *Magnetohydrodynamics*, J. Wiley Interscience, New York, 1966.
- ²⁹Marshall, W., "The Structure of Magneto-Hydrodynamic Shockwaves," *Proceedings of the Royal Society of London A*, Vol. 233, 1955, pp. 367–376.
- ³⁰Myrabo, L. N. and Razier, Y. P., "Laser-Induced Air Spike for Advanced Transatmospheric Vehicles," AIAA Paper 94-2451, American Institute of Aeronautics and Astronautics, 1994.
- ³¹Kandebo, S. W., "'Air Spike' Could Ease Hypersonic Flight Problems," *Aviation Week & Space Technology*, May 15, 1995, pp. 66–67.
- ³²Chadwick, K. M., "Shock Tunnel Experiment with Weakly Ionized Gases," *Proceedings of the 1st Workshop on Weakly Ionized Gases*, Vol. 2, Wright Laboratory Aero Propulsion and Power Directorate, Wright-Patterson AFB, OH, June 1997, pp. KK-1 – KK-34.